

## Supplementary materials

Table S1. Overview of detected m/z values for RA-PE adducts, their elemental compositions, mass shift to unmodified DOPE and proposed chemical structure.

Detected m/z	Elemental composition	Mass Accuracy (ppm)	Mass shift to unmodified DOPE	Chemical structure
744.5533	C <sub>41</sub> H <sub>79</sub> O <sub>8</sub> NP	-0.66	-	DOPE
882.6599	C <sub>50</sub> H <sub>93</sub> O <sub>9</sub> NP	1.81	(C <sub>9</sub> H <sub>14</sub> O) 138.10	HNE Schiff base
900.6708	C <sub>50</sub> H <sub>95</sub> O <sub>10</sub> NP	2.25	(C <sub>9</sub> H <sub>16</sub> O <sub>2</sub> ) 156.11	HNE Michael addition
1020.7640	C <sub>59</sub> H <sub>107</sub> O <sub>10</sub> NP	1.65	(C <sub>18</sub> H <sub>28</sub> O <sub>2</sub> ) 276.21	HNE double Schiff base
1056.7871	C <sub>59</sub> H <sub>111</sub> O <sub>12</sub> NP	3.44	(C <sub>18</sub> H <sub>32</sub> O <sub>4</sub> ) 312.23	HNE double Michael addition
880.6426	C <sub>50</sub> H <sub>91</sub> O <sub>9</sub> NP	-0.03	(C <sub>9</sub> H <sub>12</sub> O) 136.08	ONE Schiff base
858.6213	C <sub>47</sub> H <sub>89</sub> O <sub>10</sub> NP	-0.618	(C <sub>6</sub> H <sub>10</sub> O <sub>2</sub> ) 114.06	HHE Michael addition
972.6470	C <sub>53</sub> H <sub>99</sub> O <sub>12</sub> NP	1.52	(C <sub>12</sub> H <sub>20</sub> O <sub>4</sub> ) 228.09	HHE double Michael addition

Table S2. Composition of lipid bilayer membranes used in MD simulations

Bilayer composition	Number of molecules
DPPC	128
DPPC:DOPE	64:64
DPPC:HNE	128:72
DPPC:DOPE:HNE	64:64:72
DPPC:ONE	128:78
DPPC:DOPE:ONE	64:64:78
DPPC:HNE-Michael adduct	64:64
DPPC:HNE-Schiff adduct	64:64
DPPC:ONE-Schiff adduct	64:64
DPPC:HNE-Michael:HNE-Schiff adducts	64:32:32

## Supplementary Materials

### Figure description

Figure S1. Current-voltage relationships of UCP1-containing membranes measured in the absence of AA and ONE (red), in the presence of ONE (green), in the presence of AA (pink) and in the presence of ONE and AA (orange).

Figure S2. CID MS<sup>2</sup> spectrum of an ion at  $m/z$  900.67 corresponds to the HNE Michael adduct of DOPE. Product ions used for structural confirmation are marked by an asterisk (\*). R corresponds to dioleoylglycerol.

Figure S3. CID MS<sup>2</sup> spectrum of an ion at  $m/z$  882.065 corresponds to the HNE Schiff base adduct of DOPE. The product ions used for structural confirmation are marked by an asterisk (\*). R corresponds to dioleoylglycerol.

Figure S4. CID MS<sup>n</sup> spectra of DOPE modified by the HNE double Michael base adduct. A: MS<sup>2</sup> spectrum of an ion at  $m/z$  972.42 corresponds to the HNE double Michael adduct, B: MS<sup>3</sup> spectrum of an ion at  $m/z$  370.20 corresponds to the modified PE head group. The product ions used for structural confirmation are marked by an asterisk (\*). R corresponds to dioleoylglycerol, HG: phosphatidylethanolamine.

Figure S5. CID MS<sup>n</sup> spectra of DOPE modified by the HNE double Schiff base adduct. A: MS<sup>2</sup> spectrum of an ion at  $m/z$  1020.76 corresponds to the HNE double Schiff base adduct, B: MS<sup>3</sup> spectrum of an ion at  $m/z$  418.3 corresponds to the modified PE head group. The product ions used for structural confirmation are marked by an asterisk (\*). R corresponds to dioleoylglycerol.

Figure S6. CID MS<sup>2</sup> spectrum of an ion at  $m/z$  880.64 corresponds to the ONE Schiff base adduct of DOPE. The product ions used for structural confirmation are marked by an asterisk (\*). R corresponds to dioleoylglycerol.

Figure S7. CID MS<sup>2</sup> spectrum of an ion at  $m/z$  858.62 corresponds to the HHE Michael adduct of DOPE. The product ions used for structural confirmation are marked by an asterisk (\*). R corresponds to dioleoylglycerol.

Figure S8. CID MS<sup>n</sup> spectra of DOPE modified by the HHE Michael adduct. A: MS<sup>2</sup> spectrum of an ion at  $m/z$  972.42 corresponds to the HHE double Michael adduct, B: MS<sup>3</sup> spectrum of an ion at  $m/z$  370.20 corresponds to the modified PE head group. The product ions used for structural confirmation are marked by an asterisk (\*). R corresponds to dioleoylglycerol, HG: phosphatidylethanolamine.

Figure S9. RAs do not modify FA-tails of DOPE, DOPC, CL and E. coli polar lipids. The relative percentage of fatty acid methyl esters (FAME, s. Methods) was obtained from liposomes made of (in mol%) a) DOPE:DOPC:CL 45:45:10, b) DOPE:DOPC:CL 45:45:10 and 15 mol% AA c) DOPC:CL 90:10, d) DOPC:CL 90:10 and 15 mol% AA, e) E. coli polar lipid, f) E. coli polar lipid and 15 mol% AA. The concentration of HNE (violet) or ONE (yellow) was 0.84 mM.

Figure S10. (A-B) The membrane dipole modifiers, phloretin and RH421, do not influence the conductance of the membrane bilayer reconstituted with UCP1 and activated by arachidonic acid (AA). (C-D) The membrane dipole modifiers, phloretin and RH421, influence conductance of the membrane bilayer reconstituted with AA in the opposite direction. Buffer: 50 mM Na<sub>2</sub>SO<sub>4</sub>, 10 mM TRIS, 10 mM MES, 0.6 mM EGTA at pH 7.35 at T=32°C. Membrane 1,5mg/ml, UCP1 14 μg/mg, AA 15mol%. Lipid composition: DOPE, 45 mol%; DOPC, 45 mol%; CA, 10 mol%.

Figure S11. Localization of ONE revealed by molecular dynamics simulations (MD). Left - selected MD snapshots with ONE in green; middle - number density profiles for the C terminus of ONE; right - number density profiles for carbonyl (O) group of ONE. Water molecules inside the bilayer are shown in blue (OW); P\_DPPC – phosphorus atom of DPPC.

Figure S12. Calculated area per lipid in  $\text{nm}^2$  for the investigated bilayer systems.

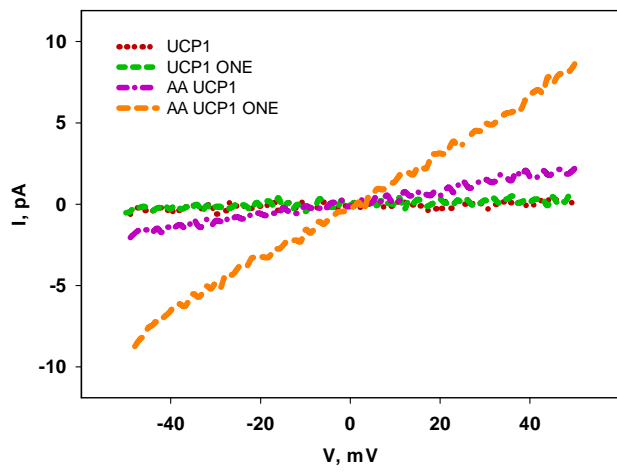


Figure S1. Jovanovic et al. (2015) Supplementary Materials

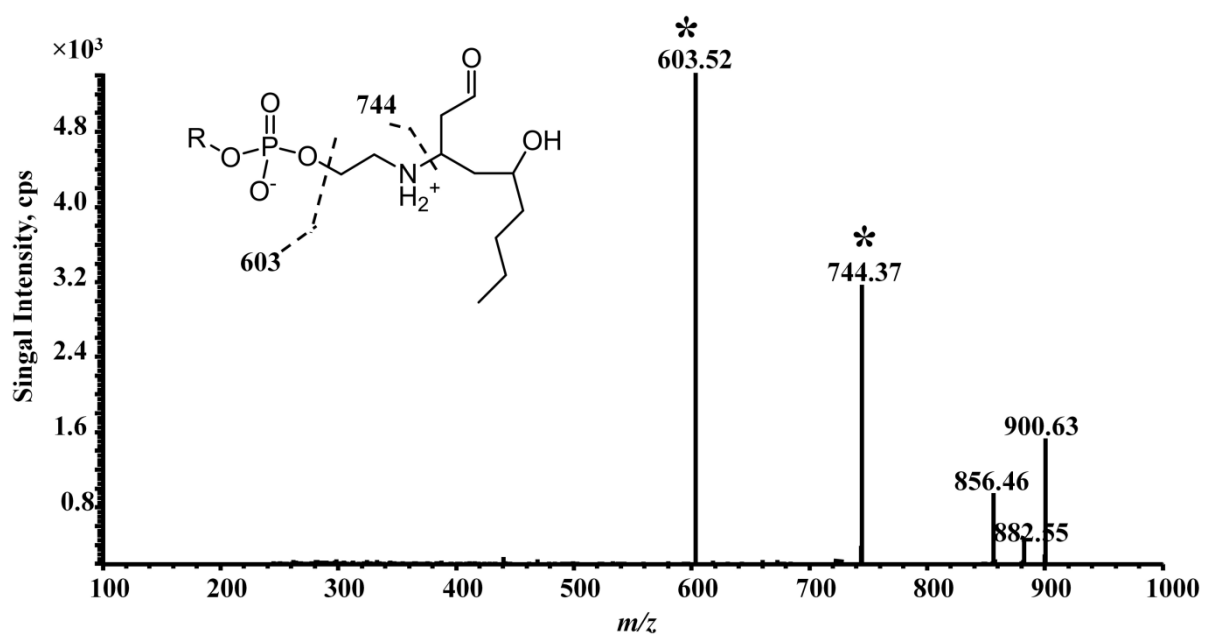


Figure S2. Jovanovic et al. (2015) Supplementary Materials

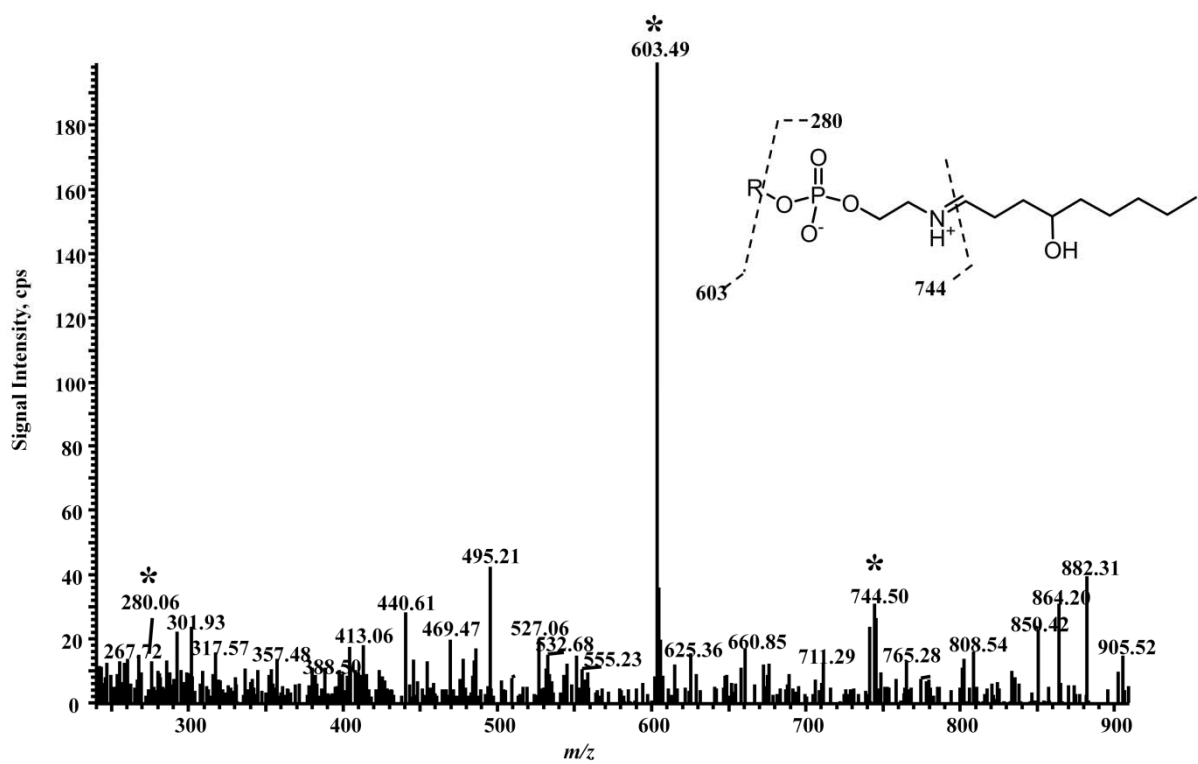


Figure S3. Jovanovic et al. (2015) Supplementary Materials

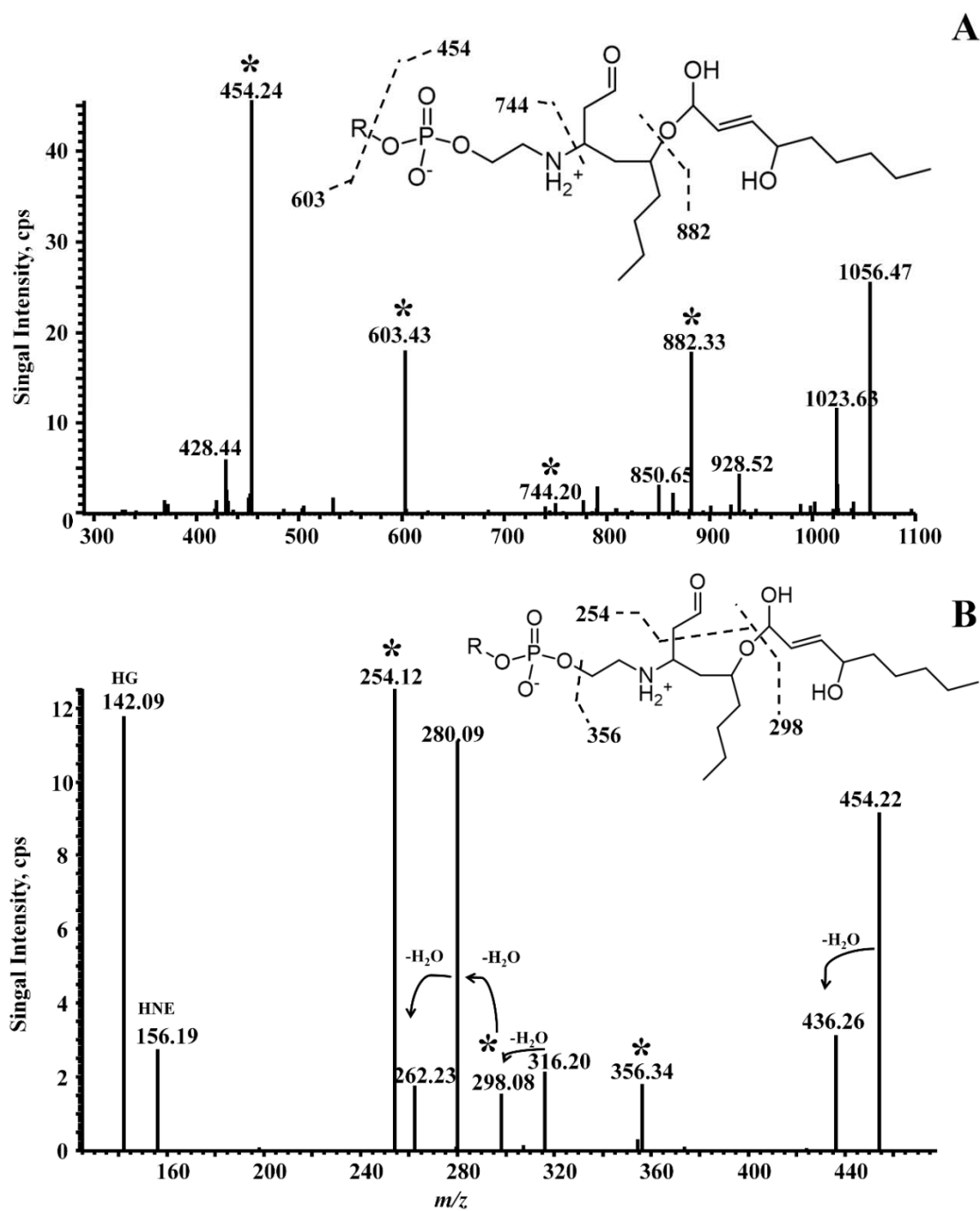


Figure S4. Jovanovic et al. (2015) Supplementary Materials



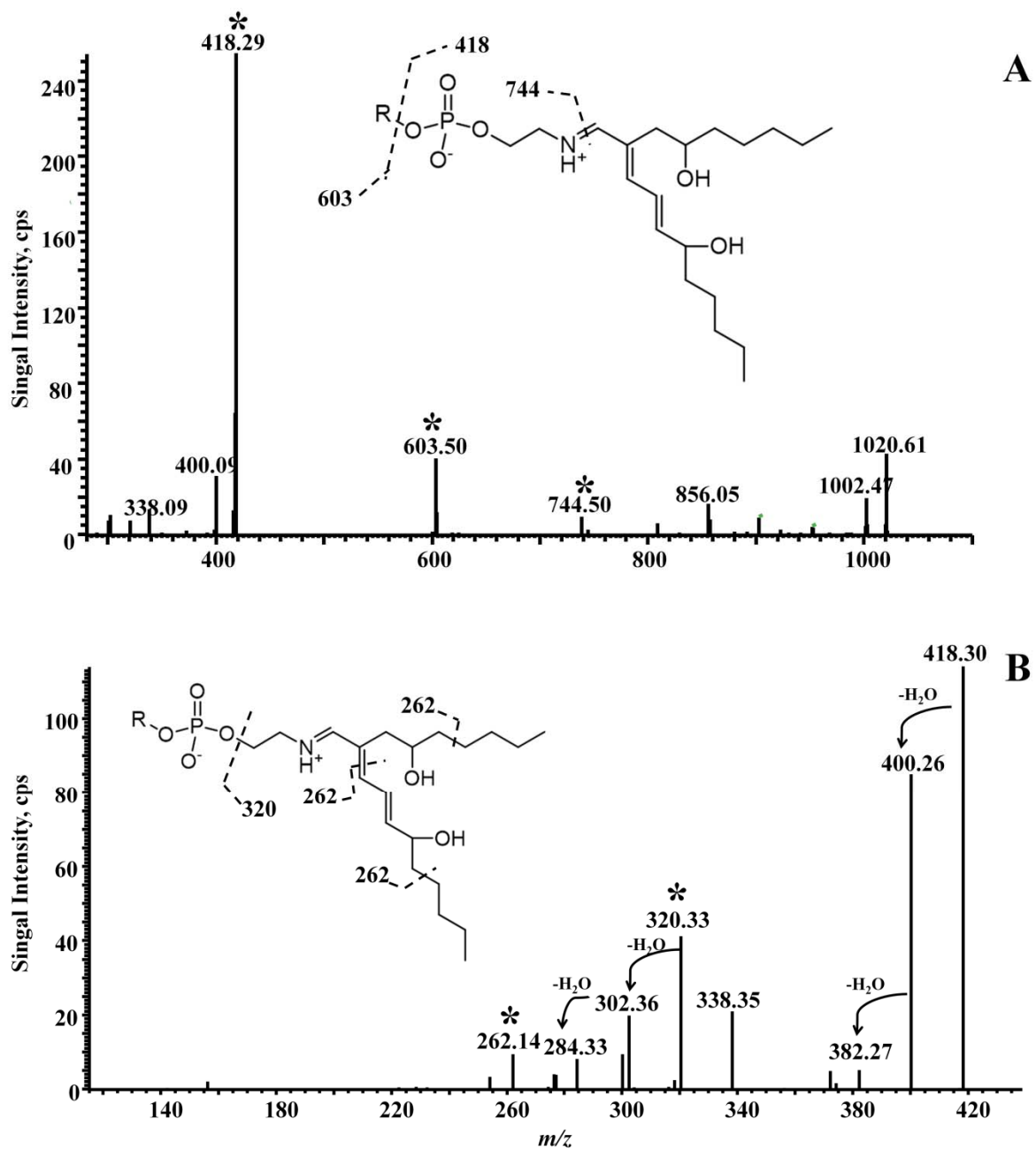


Figure S5. Jovanovic et al. (2015) Supplementary Materials

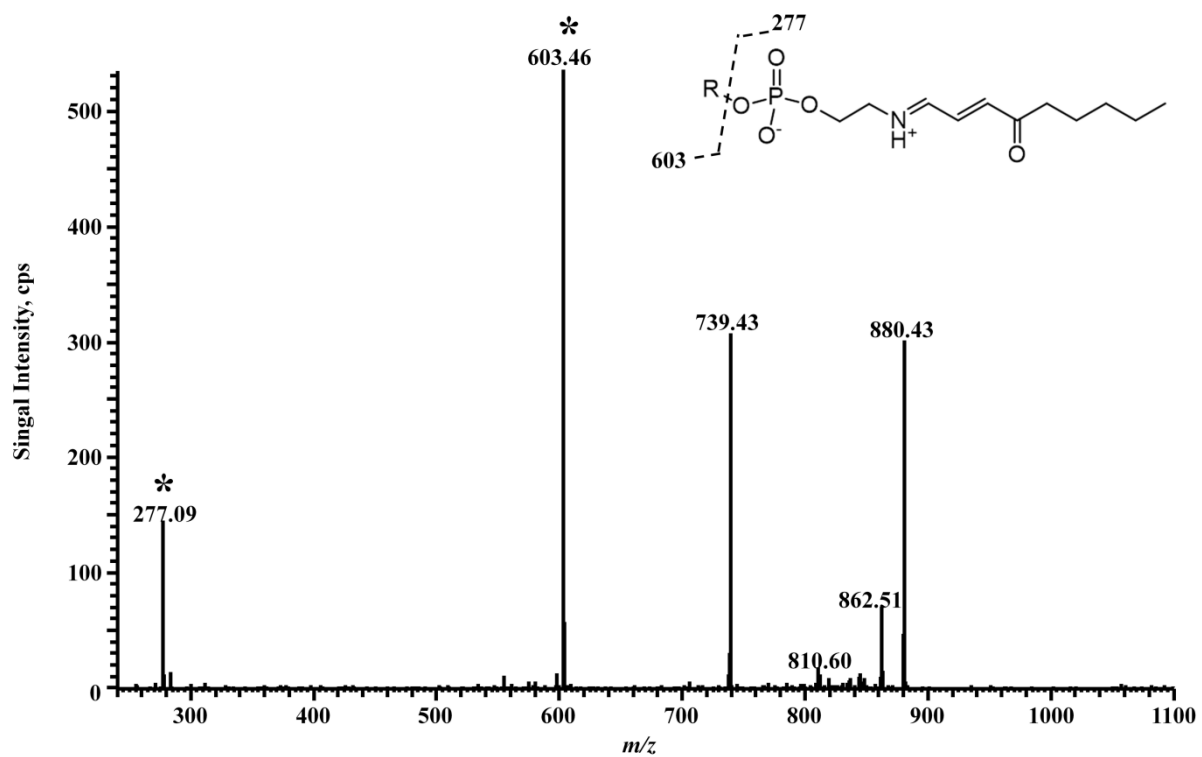


Figure S6. Jovanovic et al. (2015) Supplementary Materials

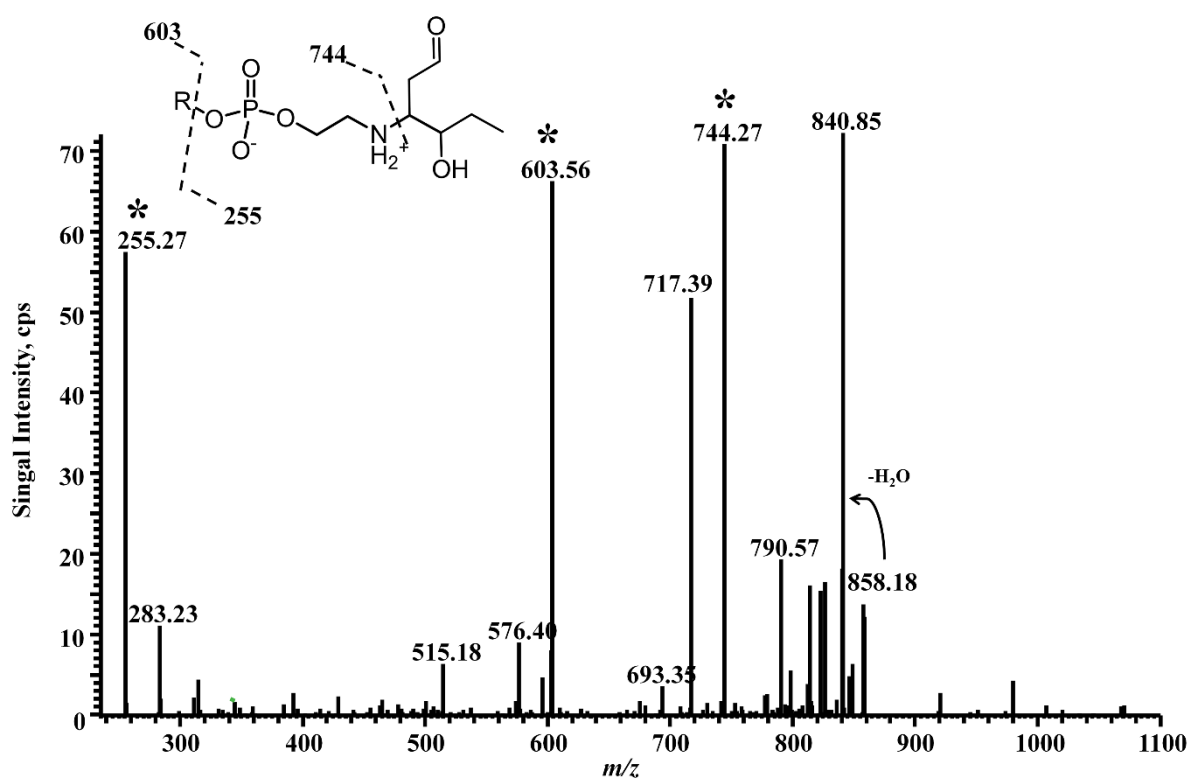


Figure S7. Jovanovic et al. (2015) Supplementary Materials

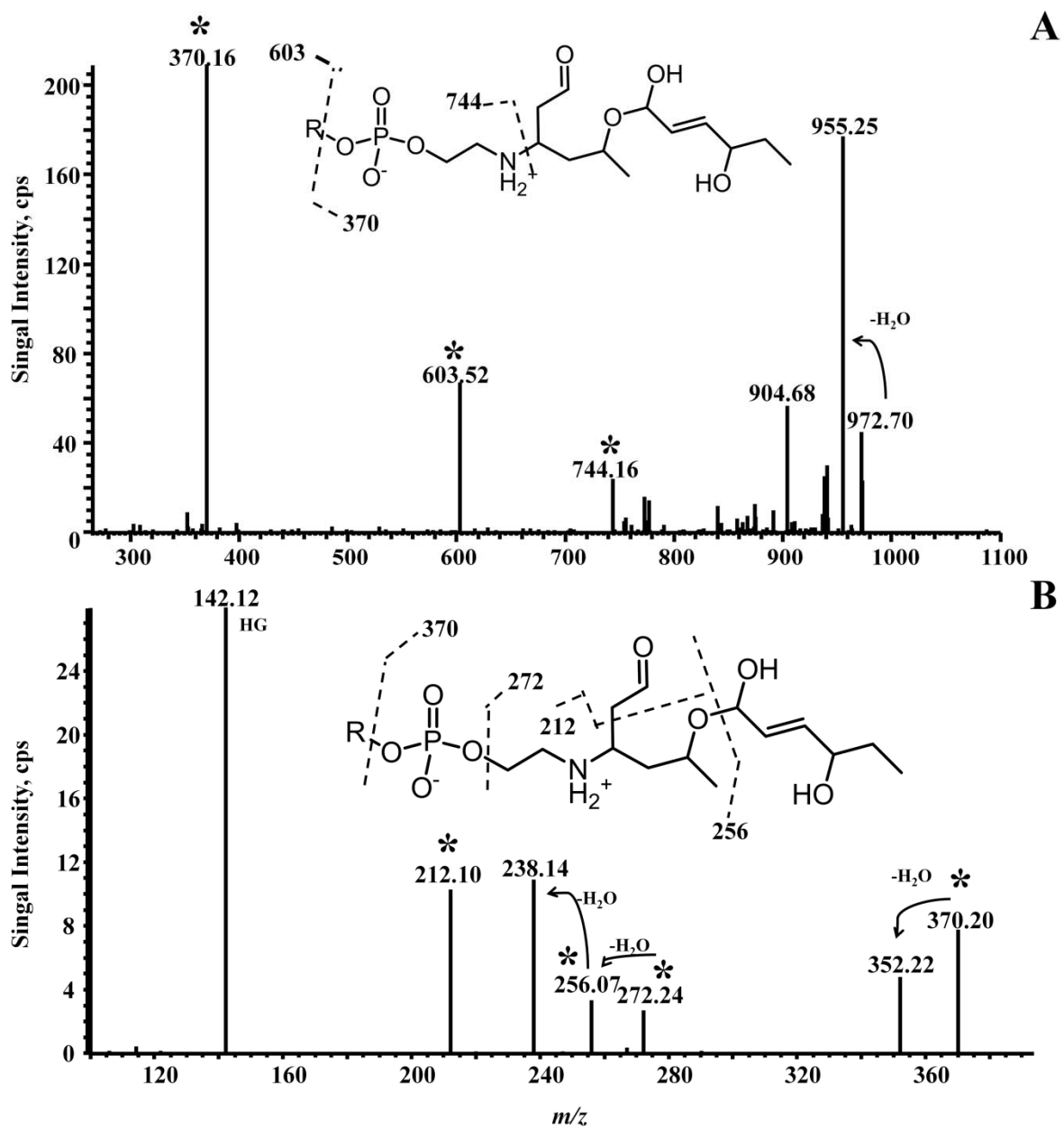


Figure S8. Jovanovic et al. (2015) Supplementary Materials

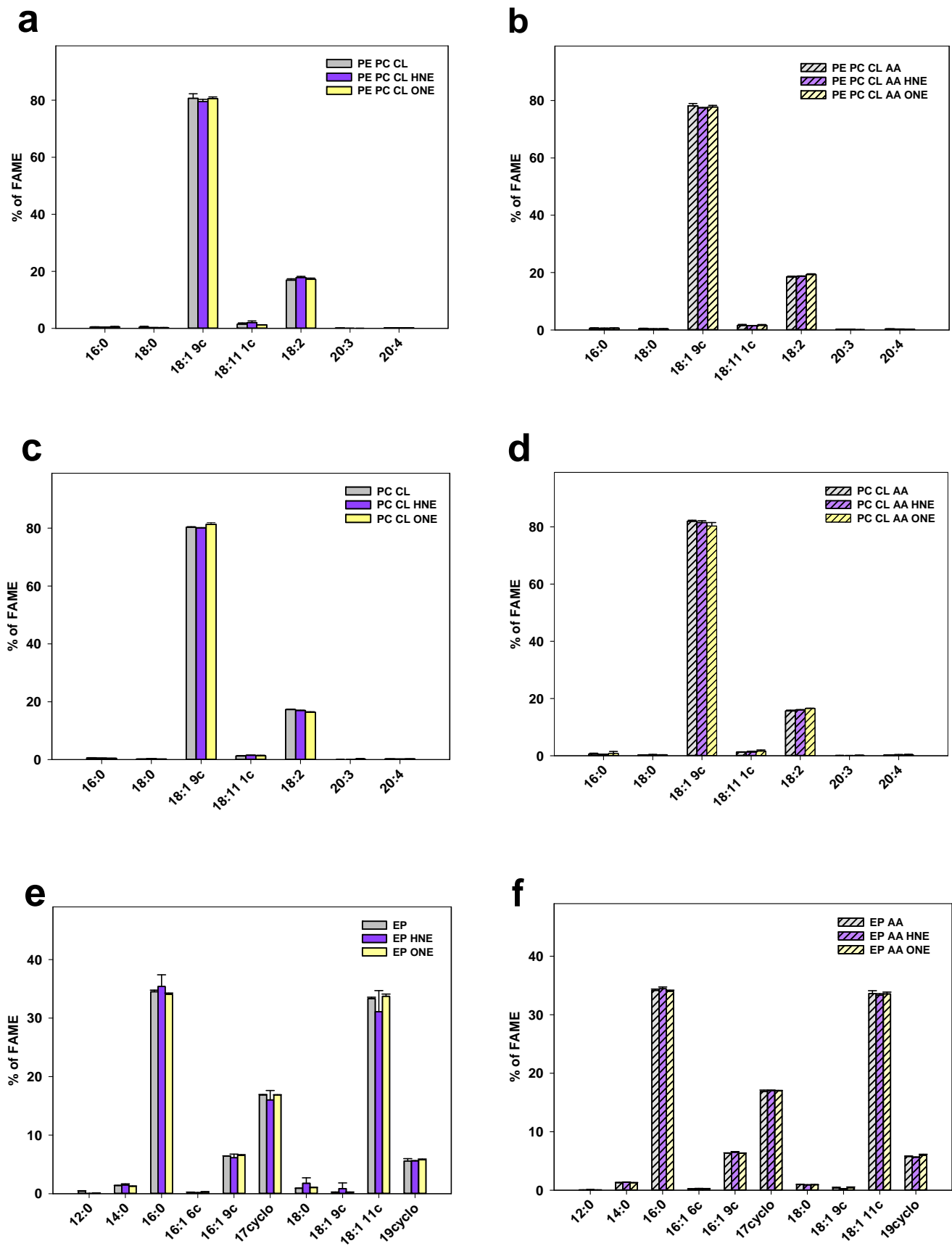


Figure S9. Jovanovic et al. (2015) Supplementary Materials

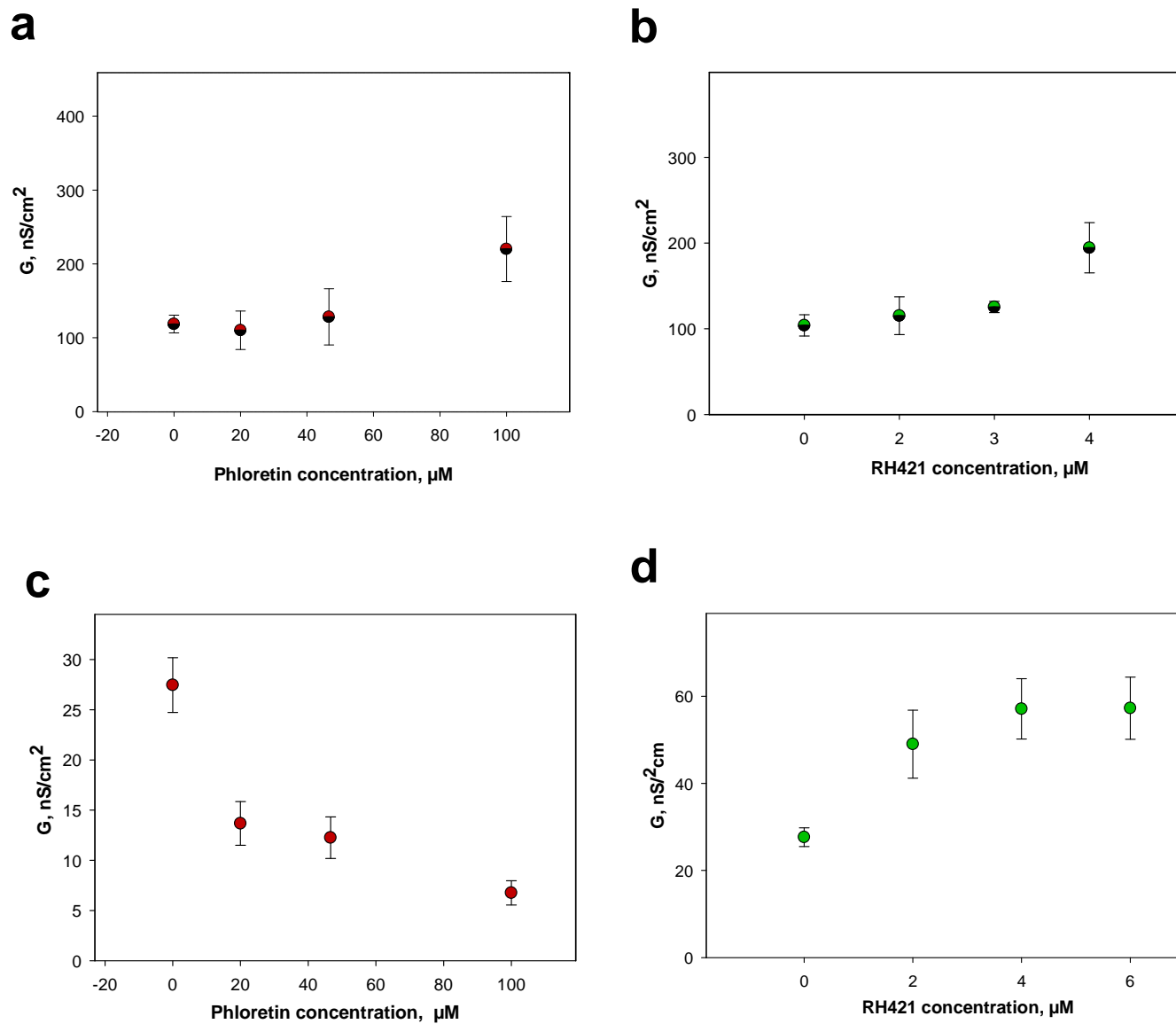


Figure S10. Jovanovic et al. (2015) Supplementary Materials

# DPPC + ONE

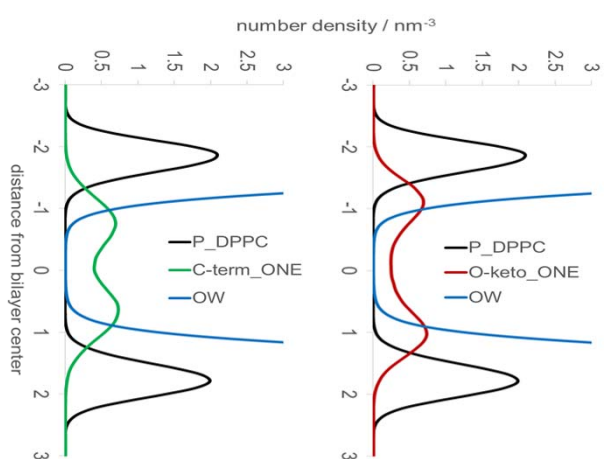
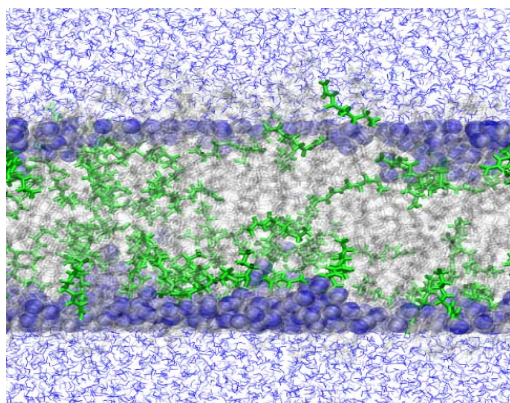
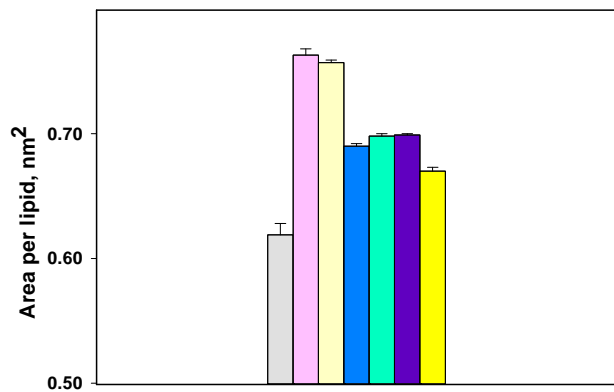


Figure S11. Jovanovic et al. (2015) Supplementary Materials



- none
- HNE
- ONE
- DPPC + HNE-Michael adduct
- DPPC + HNE-Schiff adduct
- DPPC + HNE-Michael + HNE-Schiff adduct
- DPPC + ONE-Schiff adduct

Figure S12. Jovanovic et al. (2015) Supplementary Materials